J Mol Model (2014) 20:2507
DOI 10.1007/s00894-014-2507-y

ORIGINAL PAPER

Metal-doped graphene layers composed with boron nitride–graphene as an insulator: a nano-capacitor

Majid Monajjemi

Received: 18 August 2014 / Accepted: 13 October 2014 / Published online: 31 October 2014

Abstract A model of a nanoscale dielectric capacitor composed of a few dopants has been investigated in this study. This capacitor includes metallic graphene layers which are separated by an insulating medium containing a few h-BN layers. It has been observed that the elements from group IIIA of the periodic table are more suitable as dopants for hetero-structures of the {metallic graphene/hBN/metallic graphene} capacitors compared to those from groups IA or IIA. In this study, we have specifically focused on the dielectric properties of different graphene/h-BN/graphene including their hetero-structure counterparts, i.e., Boron-graphene/h-BN/Boron-graphene, Al-graphene/h-BN/Al-graphene, Mg-graphene/h-BN/Mg-graphene, and Be-graphene/h-BN/Be-graphene stacks for monolayer form of dielectrics. Moreover, we studied the multi dielectric properties of different (h-BN)n/graphene hetero-structures of Boron-graphene/(h-BN)n/Boron-graphene.

Keywords Boron nitride–graphene · Dopant · Doped graphene · Nano-capacitor

Introduction

Graphene has a relatively flexible molecular structure due to its electronic properties. It can be chemically fitted on top of a deposit metal atom [1], a deposit molecule can be fitted on its top [2], nitrogen and boron can be incorporated in its structure [3] and can have a doped atom inside its sheet. This structure can be used in wide areas of research such as electronics, capacitor, superconductors, batteries, and diodes. The considerable characteristic of graphene is that it is a Dirac solid, with the electron energy being linearly dependent on the wave vector near the vertices of the hexagonal Brillouin zone [4]. A complete history for the rising of graphene has been given by Geim and Novoselov [5].

It is important to calculate the properties of some dopants inside the electrodes of a capacitor. Therefore we have investigated a nano-capacitor using B- and N-doped graphene bilayer samples employing different strategies for understanding their properties. The B and N atoms are the natural templates for being doped in graphene due to their similar atomic size as that of C and of their hole acceptor and electron donor characteristics for B- and N-doping substitutions, respectively.

We have simulated two configurations of doped bi-layer graphene with various atoms (between 0.5 % up to 10 % atom fraction) including horizontal boron-nitride sheets $(h\text{-}BN)_n$ (n=1, 2 and 3), (Scheme 1). The results of our simulation indicates that the configurations with dopant atoms replaced in a diagonal line are more energetically favorable, and the configuration with atoms of group IIIA (in the second and third rows) of the periodic table are much more stable in terms of binding energy (Scheme 1c). This is an indication that confirms homogeneous B-substitution might be more appropriate than other atoms such as N-substitution. The origin of this difference can be affected by the structure of B-C bond which is about 0.5 % longer than the C-C bond while N-C bond is about the same length as the C-C bond. The band-gap has widened up through the effect of B substitution doping on the structure of graphene, while the Fermi level lies in valence and conduction band.

In this study, we have made an attempt to understand the theoretical basis for the nanoscale dielectric capacitors which are superior to other systems of energy storage. In fact, capacitors at nanoscale have been developed as one of the most expecting energy storage mediums [6, 7].

M. Monajjemi (✉)
Department of Chemistry, Tehran Science and Research Branch, Islamic Azad University, Tehran, Iran
e-mail: m_monajjemi@srbiau.ac.ir

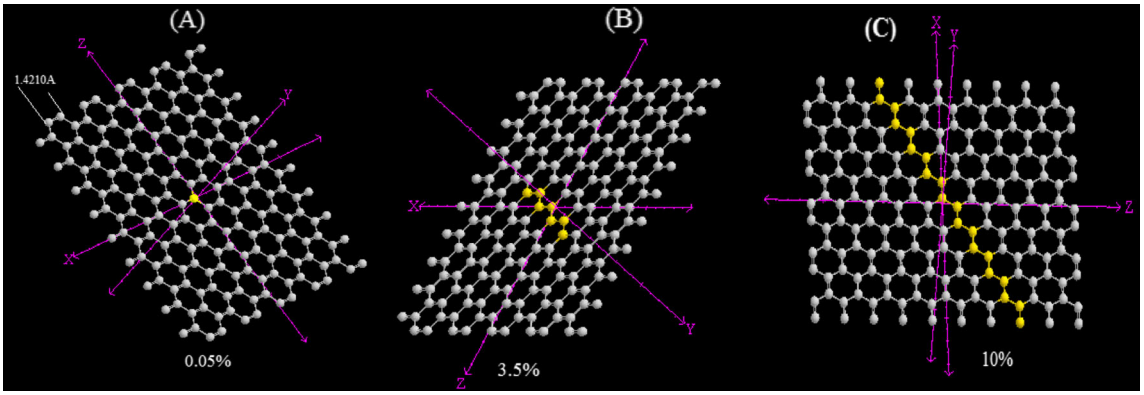

Scheme 1 Various percentages of boron dopant in graphene layers; **a**: One boron atom doped inside 200 carbons (0.5 %). **b**: Seven boron atoms doped inside 200 carbons (3.5 %). **c** Twenty boron atoms doped inside 200 carbons (10 %) in a diagonal form

Our nanoscale capacitor model is composed of hexagonal $(\text{h-BN})_n$ layers (n=1, 2, 3) which are stacked between two metal-doped graphene sheets. The single and multi-layers of $(\text{h-BN})_n$ are wide band gap insulators, so they can be applied as a dielectric material between metallic graphene layers.

The layers of h-BN can be grown on graphene layers regardless of their thickness, that have already been shown both experimentally [7, 8] and theoretically [9, 10]. It is also able to grow BN chains (perpendicular carbon atoms as well) on top of graphene and h-BN single layer [11, 12].

In this study, we have specifically focused on the dielectric properties of different $(\text{h-BN})_n$/graphene hetero-structures, including BN stacks of Al-graphene/h-BN/Al-graphene (ALGBN), B-graphene/h-BN/B-graphene (BGBN), and B-G/h-BN//h-BN/B-G {$BG(BN)_2$} with various thickness of dielectric in the insulator.

Since the main goal of using capacitors is to store energy by storing equal magnitude of electric charges of opposite sign in two electrode plates, it is important to be able to design and control the space between doped electrodes at nanoscale. Thus, by varying the separation distances and the number of h-BN, we have observed an interesting quantum size effect at small separations in our model.

Since the separation thickness of capacitor model can be as small as a nanometer at nanoscale, the stored energy has to be calculated from the first principles [12–14]. This would allow us to treat the distribution of only one kind of excess at a time, i.e., either positive or negative charge (in the same system) [13–16].

Charge separation can be achieved through applying an external electric field perpendicular to the graphene layers, simulating the operation of a capacitor by the surface charge of opposite sign initially stored on different doped plates that create a perpendicular electric field. Hence, the discharge of the capacitor due to shortening of these two plates can be prevented by placing sufficient quantity of h-BN layers between doped graphene plates.

Based on the electrostatic theory, the geometric capacitance density, C_g, is related to the applied voltage, ΔV_{app} as observed in Eq. 1:

$$C_g = \frac{\sigma}{\Delta V_{app}} = \frac{\varepsilon_r \varepsilon_{0\,A}}{d}, \tag{1}$$

where σ is the surface charge density, ε_r and ε_0 are the dielectric constant and the absolute permittivity, respectively.

A significant increase in capacitance below a thickness of 5 nm was found by Ajayan and coworkers [17] which is more than what was predicted by classical electrostatics. This unusual increase in capacitance is due to the negative quantum capacitance that these particular material systems exhibit.

Based on the percentage of B dopant and thickness of h-BN layers, we have found a significant increase in capacitance and negative quantum capacitance.

Theoretical background and model

Nano-dielectric-capacitor model has been successfully used to simulate stacking structures of graphene/h-BN/graphene [18]. Ajayan and coworkers have investigated the patterns of negative quantum effects in the interaction between the gold electrodes and h-BN films. They have determined the dielectric permittivity as a function of dielectric size via ab-inito calculations using the SIESTA atomistic simulation package [17].

Density functional theory with the van der Waals density functional for the exchange-correlation energies of Au and h-BN have been employed via a relativistic pseudo-potential in their models [19–21].

We have considered two isolated metal-doped-graphene layers which are charged by Q electrons {(and also per primitive unit-cell) (±σ)}. A nano dielectric model with $(\text{h-BN})_n$

layers (n=1, 2, 3) as a dielectric is covered by two parallel metal-doped graphene (metal=Mg, Al, Si, B) layers.

In our model, the interlayer distance for h-BN varies from a range of {3.0–5.0} Å, which are in reasonable values and agreement with the corresponding experimental (3.306 Å) [22] and theoretical amounts [23, 24].

The hybrid and quantum capacitances are related to the net capacitance, C, through the relation indicated in Eq. 2:

$$\frac{1}{C}=\frac{1}{C_g}+\frac{2}{C_Q}, \tag{2}$$

where the value of C_Q is several orders of magnitude greater than that of C_g, and hence its effect usually appears only in a very small system [17].

Ajayan and coworkers have explained [7, 16, 22, 24] the observed abnormal increase in capacitance with decreasing size, suggesting the quantum capacitance is negative for nano-systems. This effect arises from many-body interactions due to the decrease in the chemical potential of the electrons with increase of electron density.

A capacitance of radial quantum dots was reported by Maccuci and coworkers [26, 27] while Wang et al., has investigated the non-linear quantum capacitance [28] as well as the capacitance of atomic junctions [29].

The quantum mechanics component is a development model of the density of states (DoS) of the metal electrodes, and their Thomas-Fermi screening lengths. Hence, the hybrid capacitance of any nano-capacitor architecture is given as:

$$\frac{1}{C_t}=\frac{1}{C_{Q_1}}+\frac{1}{C_{Q_2}}+\frac{1}{C_g}, \tag{3}$$

where C_t is the total capacitance of the nano-capacitor, Cg is the classical (geometric) capacitance, C_{Q_1} , and C_{Q2} are the quantum capacitances due to the finite DoS of the metal doped graphene electrodes M_1G, and M_2G, respectively.

If the $C_{Q_1}\cong C_{Q_2}\equiv C_Q$ then:

$$C_Q=\frac{(\varepsilon_{metal})\varepsilon_0 A}{r_{(thomas-fermi)}\sqrt{\varepsilon_{metal}}} \tag{4}$$

which

$$r_{(thomas\ -\ fermi)}=\sqrt{\frac{\varepsilon_0}{e^2 D\left(\mu_f\right)}} \tag{5}$$

$$D\left(\mu_f\right)=\frac{d_n}{d_{\mu_1}}=\frac{d_n}{d_{\mu_2}}\left(J.m^3\right)^{-1}, \tag{6}$$

where D is the DoS at the Fermi level [30, 31] of either electrode and

$$r_{(thomas-fermi)}=3.39.10^{-9}\sqrt{\frac{r_s}{a_0}} \tag{7}$$

which $\frac{r_s}{a_0}=3.01$ for metal=Au [31].

Hence, the hybrid capacitance due to the composition of both classical and quantum capacitances is:

$$C_t=(2\gamma+1)^{-1}C_g And\gamma=\frac{r(thomas-fermi)}{d}\left(\frac{\varepsilon_r^2}{\varepsilon_{metal}}\right)^{-1}. \tag{8}$$

Computational details

All the calculations were performed by GAMESS-US package [32]. We have mainly focused on getting the results from DFT methods such as m062x, m06-L, and m06 for the non-bonded interaction of Al-G/h-BN/Al-G (ALGBN), B-G/h-BN/B-G (BGBN), and B-G/h-BN//h-BN/B-G {$BG(BN)_2$} which are monotonous through the comparison between different situations.

The m062x, m06-L, and m06-HF are rather new DFT functionals with a good correspondence in non-bonded calculations and are useful for the energies of distance between two fragments in a capacitor; for a medium of ~3–5 Å, and long ranges of dielectric thickness (≥ 5 Å) [33].

We employed density functional theory with the van der Waals density functional to model the exchange-correlation energies of doped graphene and h-BN [19]. The double ζ-basis set with polarization orbitals (DZP) were used for doped graphene atoms while single ζ-basis sets with polarization orbitals (SZP) were employed for the h-BN layers, respectively.

For non-covalent interactions, the B3LYP method is unable to describe van der Waals [33, 34] capacitor systems by medium-range interactions such as the interactions of two electrodes and dielectric sheets. The B3LYP and most other popular functionals are insufficient to illustrate the exchange and correlation energy for distant non-bonded medium-range systems correctly (such as two electrodes and dielectric thickness in a capacitor). Moreover, some recent studies have shown that inaccuracy for the medium-range exchange energies leads to large systematic errors in the prediction of molecular properties [35–39].

Graphene is known to relax in 2-D honeycomb structures and the B and N doped graphene will be assumed to have similar structure, unless they are violated by energy minimization considerations. A monolayer of G containing 76 atoms with zigzag edges was optimized and allowed to relax to its minimum energy structure. The edges were saturated with hydrogen atoms to neutralize the valance of terminal carbons,

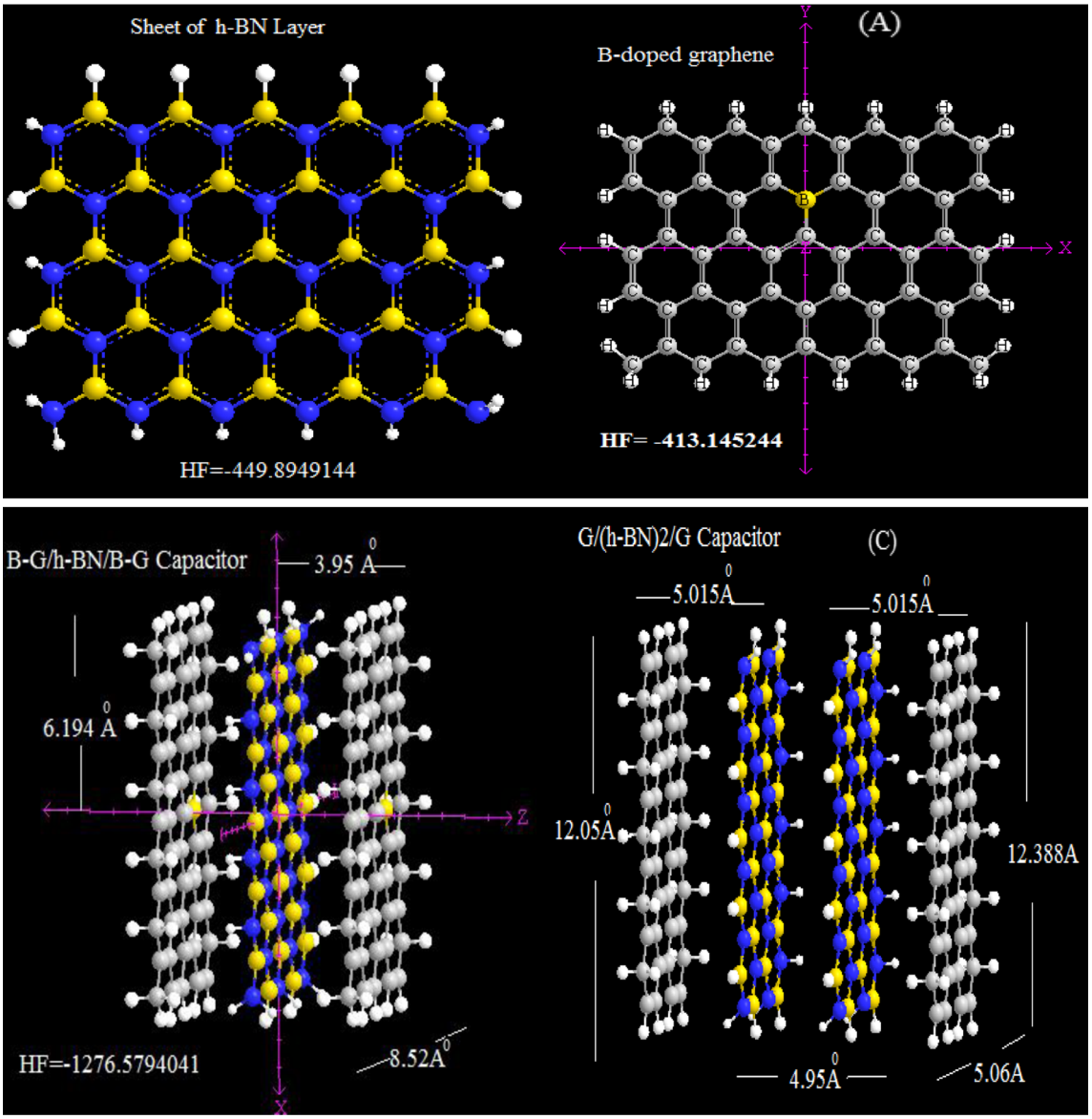

Scheme 2 Two models of nano-capacitors with different sizes

reducing the edge effects after relaxation. All C-C-C angles were calculated to be about 120 and all the C-C and C-H bound lengths were about 1.421 and 1.085, respectively which are in good agreement with reported values [40].

Table 1 The charges of two electrodes and the stability energy of capacitors

"Capacitor" various dopants	$\frac{1}{2}$ *Dielectric thickness* (Å)	$\Delta E_S(eV)=$	q^{+}_{m-G}	q^{-}_{m-G}	q_{h-BN}
AlGBN	3.8	−48.25	+0.25	−0.19	−0.06
AlGBN	3.95	−46.85	+0.18	−0.15	−0.03
AlGBN	4.5	−44.88	+0.015	−0.014	−0.001
AlGBN G	5.0	−44.88	+0.005	−0.004	−0.001
BGBN	3.95	−10.72	+0.15	−0.10	−0.05
G/h-BN/ G	3.95	−1.49	+0.000	0.000	0.000
SiGBN	3.95	−1.85	+0.03	−0.02	−0.01
MgGBN	3.95	−8.90	+0.09	−0.09	0.00
BegBN	3.95	−2.10	+0.02	−0.03	0.01

Table 2 The charges of two electrodes including two dielectrics in various thicknesses of boron dopants

Capacitor	$\frac{1}{2}Dielectric\ thickness(\text{Å})$	ΔE_S (eV)	q^{+}_{B-G}	q^{-}_{B-G}	$(q_{h-BN})_1$	$(q_{h-BN})_2$	Gap Energy(eV)
B-G/h-BN//h-BN/B-G	7.5	−8.70	+0.18	−0.14	−0.02	−0.02	−0.92
B-G/h-BN//h-BN/B-G	6.0	−10.78	+0.28	−0.24	−0.02	−0.02	−1.13
B-G/h-BN//h-BN/B-G	5.5	−13.65	+0.31	−0.29	−0.01	−0.01	−1.30
B-G/h-BN//h-BN/B-G	5.0	−25.97	+0.39	−0. 37	−0.01	−0.01	−1.36
B-G/h-BN /B-G	3.95	−10.72	+0.15	−0.10	−0.05	-	−1.58
G/h-BN//h-BN/G	7.5	−0.06	+0.002	−0.002	−0.00	−0.00	−4.72

Geometry optimizations and electronic structure calculations have been carried out using the m06 (DFT) functional. This approach is based on an iterative solution of the Kohn-Sham equation [41] of the density functional theory in a plane-wave set with the projector-augmented wave pseudo-potentials. The Perdew-Burke-Ernzerhof (PBE) [42] exchange-correlation (XC) functional of the generalized gradient approximation (GGA) is adopted. The optimizations of the lattice constants and the atomic coordinates are made by the minimization of the total energy. The dimension of the capacitor has been set to 12.388×3.95×8.52 Å (Scheme 2) and the sheets are separated by various distances (Tables 1 and 2) along the perpendicular direction to avoid interlayer interactions. During the calculation processes, except for the band determination, the partial occupancies were treated using the tetrahedron methodology with Blöchl corrections [43].

For geometry optimizations, all the internal coordinates were relaxed until the Hellmann-Feynman forces were less than 0.005 Å. We further calculated the interaction energy between the B-G electrodes and h-BN sheet in the structures (The number of h-BN layers was varied to examine size-dependent electrical properties). The dielectric permittivity as a function of dielectric size was determined via ab-inito calculations.

In our model, the electrodes have been doped by various percentages of boron atoms which are likely to be adjusted by the surrounding host C atoms. Therefore, when the graphene sheet is doped with one boron atom, the boron atom also undergoes the sp^2 hybridization. Due to the relatively similar size of C and B, no significant distortion in 2-D structure of graphene is expected, except for the change in adjoining the bond length. As a result, a bond length is found to expand to 1.48 Å. Using the computational procedure as stated above, the electronic properties, especially the band structure can be calculated.

By doping boron atoms in graphene, Fermi level shifts significantly below the Dirac point resulting in a p-type doping. This would break the symmetry of graphene into two graphene sub-lattices due to the presence of the B atoms which would eventually lead toward a change of the behavior of graphene from semimetal to conductor.

The charge transfer and electrostatic potential-derived charge were also calculated using the Merz-Kollman-Singh [44], chelp [45], or chelpG [46].

The charge calculation methods based on molecular electrostatic potential (MESP) fitting are not well-suited for treating larger systems whereas some of the innermost atoms are located far away from the points at which the MESP is computed.

In such a condition, variations of the innermost atomic charges will not lead toward a significant change of the MESP outside of the molecule, meaning that the accurate values for the innermost atomic charges are not well-determined by MESP outside the molecule [47].[1] The representative atomic charges for molecules should be computed as average values over several molecular conformations.

A detailed overview of the effects of the basis set and the Hamiltonian on the charge distribution can be found in [48–51]. We have also extracted the charge density profiles from first-principles calculation through an averaging process described in [52].

Although infinite graphene sheets are intrinsically metallic, our B-G system exhibits an enhancement in the metallic properties. The interaction energy for capacitor was calculated in all items according to Eq. 9:

$$\Delta E_S(eV) = \left\{E_C - \left(2E_{Dopant-G} + E_{h-BN}\right)\right\} + E_{BSSE}, \qquad (9)$$

where the ΔE_S is the stability energy of capacitor.

Results and discussion

In this study, we specifically studied the dielectric properties of different h-BN/graphene of G/**h-BN**/G (GBN) including hetero-

[1] In the CHELPG (Charges from Electrostatic Potentials using a Grid based method), atomic charges are fitted to reproduce the molecular electrostatic potential (MESP at a number of points around the molecule. The MESP is calculated at a number of grid points spaced 3.0 pm apart and distributed regularly in a cube. Charges derived in this way don't necessarily reproduce the dipole moment of the molecule. CHELPG charges are frequently considered superior to Mulliken charges as they depend much less on the underlying theoretical method used to compute the wave function (and thus the MESP).

Table 3 The dielectric and capacitance of modeled capacitors in various thicknesses

Capacitor	$\frac{1}{2}$ *Dielectric thickness* (Å)	$\Delta(V^{(1)}_{(B-G)})-V^{(2)}_{(B-G)}))$ (a.u.)	$C(F)\times 10^{21}$	k
B-G/h-BN//h-BN/B-G	7.5	(−1718.4+1721.3)=2.9	7.7	2.13
B-G/h-BN//h-BN/B-G	6.0	(−1845.2+1848.7)=3.5	10.9	2.43
B-G/h-BN//h-BN/B-G	5.5	(−1804.1+1808)=3.9	11.89	2.40
B-G/h-BN//h-BN/B-G	5.0	(−1968.2+1973.2)=5.0	11.74	2.17
B-G/h-BN /B-G	3.95	(−3481.3+3483.8)=2.5	6.4	1.07
G/h-BN//h-BN/G	7.5	(−1713.8+1715.6)=1.8	0.01	~

structures, BG/h-BN/BG (BGBN), AlG/h-BN/AlG (AlGBN), MgG/h-BN/MgG (MgGBN), and BeG/h-BN/BeG (BeGBN) stacks for monolayer of dielectric. Moreover, we have investigated the multi dielectric properties of different $(h\text{-}BN)_n$/graphene hetero-structures of BG/$(h\text{-}BN)_n$/BG[BG$(BN)_n$].

Since the h-BN in nature is an ideal electrical insulator that can be polarized by applying an external electric field, the number of BN layers between the graphene plates have been calculated and optimized as a suitable dielectric. Being an excellent spacer with a lattice constant close to that of graphene, BN was chosen as a dielectric. Furthermore, graphene and h-BN are two well-known single layer honeycomb structures, so the proposed model can be easily fabricated.

The values of the distance between graphene layers capping h-BN layers, dielectric constants of the layered h-BN sheets (k), magnitude of the charges on the graphene plates, the stability energy of capacitor (in eV), and the potential difference between the electrodes of graphene plates are listed in Tables 1, 2, and 3.

Various dopants in Table 1 indicate proper situations for boron and aluminum dopants in graphene electrodes.

In addition, according to electronic structures we have considered two isolated graphene layers which are doped by

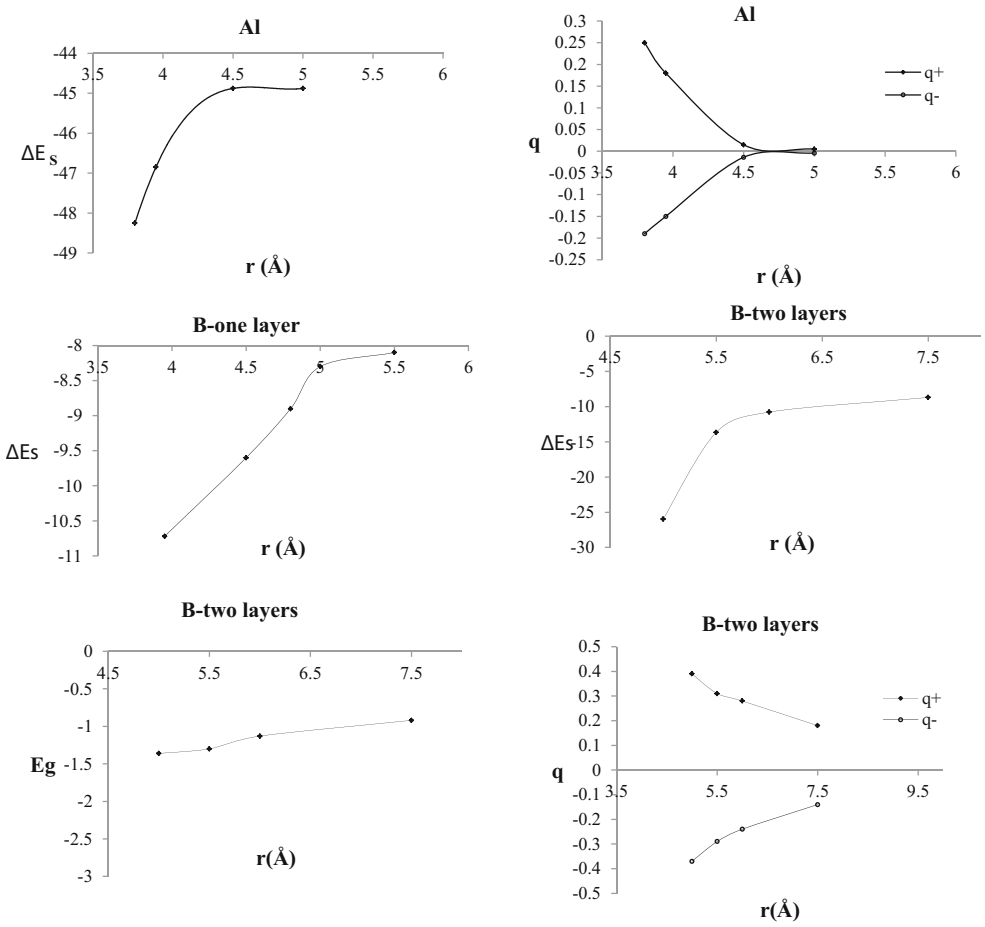

Fig. 1 Total charges of each electrode, the stability (**ΔEs**), and gape (**Eg**) energies of aluminum and boron dopants versus distance changing

boron atoms in various distances. They have been charged by q^{+}_{m-G} and $q^{-}_{(m-G)}$ coulombs as shown in Table 1.

The atomic structures, interlayer spacing, relative positions of the layers and the cell parameters have been optimized. The potential energy difference between the two graphene layers, $V=\Delta(V^{(1)}_{B-G}-V^{(2)}_{B-G})$ (a.u.) are depicted in Table 3 and varies between 1.8 and 5 V, which leads to the accumulation of a near equal amount of surface charges of the opposite sign.

The plots of the negative and positive charges for the doped-graphene layers are shown in Fig. 1, where the best symmetry charges for the electrodes are around 7.5 and 4.5 Å for boron and aluminum, respectively.

Although the dielectric strength can be deduced from the band structure of BN spacer, here we have calculated the dielectric constant straightaway from Eq. 1 that is much more accurate than the other methods.

It is arguable that for BN spacer consisting of a few layers, the different voltages between two electrodes depend on various conditions such as non-equilibrium state, the coupling between graphene and adjacent h-BN, etc. requiring a thorough analysis.

For the nanoscale BGBN and planar capacitor, the different voltages can be estimated from the band gap. This amount is 2.5 V for a single layer of h-BN (Table 3). Approximately, the relative permittivity of a $(h\text{-}BN)_2$ dielectric can be almost twice as high compared to the monolayer boron nitride (Table 3).

The comparison among the stability ΔE_S (eV) and energy gap (eV) of various thicknesses which indicates a straight relation between ΔE_S and energy gap (E_g) have been shown in Fig. 1 and Table 2.

Table 3 indicates the small value of the capacitance for single h-BN layer which passes through a maximum amount for $(h\text{-}BN)_2$ and then decreases by falling the distance.

For long distances of dielectric thickness, the classical capacitance rule of the $C \propto \frac{1}{d}$ is adaptable. This adaptability does not go for short distances, which is attributed to the quantum size effect.

In addition our system can be extended based on the result of using the electrostatic potentials on the inner and outer surfaces of a group of carbon and B x N x model nanotubes [53].

Conclusions

In this study, we have shown the model of a nanoscale dielectric capacitor composed of a few dopants including metallic graphene layers separated by an insulating medium containing a few h-BN layers. We have exhibited that in this model, the dopants from IIIA main group (the second and third rows) of the periodic table are the suitable dopants for hetero-structures of the metal-G/hBN/metal-G capacitor rather than IA or IIA main groups.

The capacitor with two layers of h-BN has a high dielectric constant compared to one layer of h-BN. Our theoretical results show that the relative permittivity of a $(h\text{-}BN)_2$ dielectric can be almost twice as high compared to the monolayer boron nitride.

There is a straight relation between ΔE_S and energy gap (E_g) in all models of metal-dopant capacitors.

References

1. Ostinga JB, Heersche HB, Liu X, Morpuzo AF, Vanderspyen LMK (2008) Gate-induced insulating state in bilayer graphene devices. Nat Mater 7:151–157
2. Dressalhaus MS, Dresselhaus G, Eklunch PC (1995) Academic, San Diego
3. Tanuma S, Kanimura H (1985) Overview on the progress of graphite intercalation compound research project. Progress of research in Japan. World Scientific, Singapore
4. Castro Neto AH, Guinea F, Peres NMR, Novoselov KS, Geim AK (2009) The electronic properties of graphene. Rev Mod Phys 81(1):109
5. Geim AK, Novoselov KS (2007) The rise of graphene. Nat Mater 6(3):183–191
6. Yildirim T, Ciraci S (2005) Titanium-decorated carbon nanotubes as a potential high-capacity hydrogen storage medium. Phys Rev Lett 94:175501
7. Durgun E, Ciraci S, Zhou W, Yildirim T (2006) Transition-metal-ethylene complexes as high-capacity hydrogen-storage media. Phys Rev Lett 97:226102
8. Liu Z, Song L, Zhao SZ, Huang JQ, Ma LL, Zhang JN, Lou J, Ajayan PM (2011) Direct growth of graphene/hexagonal boron nitride stacked layers. Nano Lett 11:2032–2037
9. Özçelik VO, Cahangirov S, Ciraci S (2012) Epitaxial growth mechanisms of graphene and effects of substrates. Phys Rev B 85:235456
10. Sachs B, Wehling TO, Katsnelson MI, Lichtenstein AI (2011) Adhesion and electronic structure of graphene on hexagonal boron nitride substrates. Phys Rev B 84:195414
11. Monajjemi M, Boggs JE (2013) A new generation of BnNn rings as a supplement to boron nitride tubes and cages. J Phys Chem A 117: 1670–1684. doi:10.1021/jp312073q
12. Ataca C, Ciraci S (2011) Perpendicular growth of carbon chains on graphene from first-principles. Phys Rev B 83:235417
13. Chan KT, Lee H, Cohen ML (2011) Gated atoms on graphene studied with first-principles calculations. Phys Rev B 83:035405
14. Chan KT, Lee H, Cohen ML (2011) Phys Rev B 84:165419
15. Suarez AM, Radovic LR, Bar-Ziv E, Sofo JO (2011) Gate-voltage control of oxygen diffusion on graphene. Phys Rev Lett 106:146802
16. Topsakal M, Ciraci S (2012) Effects of static charging and exfoliation of layered crystals. Phys Rev B 85:045121
17. Shi G, Hanlumyuang Y, Liu Z, Gong Y, Gao W, Li B, Kono J, Lou J, Vajtai R, Sharma P, Pulickel M, Ajayan PM (2014) Boron nitride–graphene nano-capacitor and the origins of anomalous size-dependent increase of capacitance. Nano Lett 14:1739–1744
18. Ozcelik VO, Ciraci SJ (2013) Size dependence in the stabilities and electronic properties of α-graphyne and its boron nitride analogue. Phys Chem C 117(5):2175–2182
19. Dion M, Rydberg H, Schroder E, Langreth DC, Lundqvist BI (2004) Van der Waals density functional for general geometries. Phys Rev Lett 92:24640

20. Monajjemi M (2013) Non bonded interaction between BnNn (stator) and image (rotor) systems: a quantum rotation in IR region. Chem Phys 425:29–45
21. Gao M, Lyalin A, Taketsugu TJ (2012) Catalytic activity of Au and Au_2 on h-BN surface adsorption and activation of O_2. Phys Chem 116:9054–9062. doi:10.1021/jp300684v#_blank
22. Paszkowicz W, Pelka JB, Knapp M, Szyszko T, Podsiadlo S (2002) Lattice parameters and anisotropic thermal expansion of hexagonal boron nitride in the 10–297.5 K temperature range. Appl Phys A 75(3):431–435
23. Hamada I, Otani M (2010) Comparative van der Waals density-functional study of graphene on metal surfaces. Phys Rev B 82:153412
24. Liu Z, Zhan YJ, Shi G, Moldovan S, Gharbi M, Song L, Ma LL, Gao W, Huang JQ, Vajtai R, Banhart F, Sharma P, Lou J, Ajayan PM (2012) Anomalous high capacitance in a coaxial single nanowire capacitor. Nat Commun 3:879
25. Liu Z, Ma LL, Shi G, Zhou W, Gong YJ, Lei SD, Yang XB, Zhang JN, Yu JJ, Hackenberg KP, Babakhani A, Idrobo JC, Vajtai R, Lou J, Ajayan PM (2013) In-plane heterostructures of graphene and hexagonal boron nitride with controlled domain sizes. Nat Nanotechnol 8(2):119–124
26. Macucci M (1997) Differential capacitance between circular stacked quantum dots. Phys E 1:7–14
27. Macucci M, Hess K, Iafrate GJ (1993) Electronic energy spectrum and the concept of capacitance in quantum dots. Phys Rev B 48: 17354–17363
28. Wang B, Zhao X, Wang J, Guo H (1999) Nonlinear quantum capacitance. Appl Phys Lett 74:2887–2889
29. Wang J et al (1998) Capacitance of atomic junctions. Phys Rev Lett 80:4277–4280
30. Mulak J (1996) The Thomas–Fermi type screening of the crystal field multipole moments. J Solid State Chem 124:182–189
31. Ashcroft NW, Mermin ND (1976) Solid state physics. Saunders College Publishing, Philadelphia
32. Schmidt MW, Baldridge KK, Boatz JA, Elbert ST, Gordon MS, Jensen JH, Koseki S, Matsunaga N, Nguyen KA et al (2004) General atomic and molecular electronic structure system. J Comput Chem 14(11):1347–1363. doi:10.1002/jcc.540141112
33. Zhao Y, Truhlar DG (2008) The M06 suite of density functionals for main group thermochemistry, thermochemical kinetics, noncovalent interactions, excited states, and transition elements: two new functionals and systematic testing of four M06-class functionals and 12 other functionals. Theory Chem Account 120:215–241. doi:10.1007/s00214-007-0310-x
34. Zhao Y, Truhlar DG (2008) Density functionals with broad applicability in chemistry. Acc Chem Res 41(2):157–167
35. Monajjemi M, Jafari Azan M, Mollaamin F (2013) Density functional theory study on B30N20 nanocage in structural properties and thermochemical outlook. Fuller Nanotub Car N 21(6):503–515
36. Grimme S (2006) Seemingly simple stereo electronic effects in alkane isomers and the implications for Kohn–Sham density functional theory. Angew Chem Int Ed 45:4460–4464. doi:10.1002/anie.200600448
37. Monajjemi M, Seyed Hosseini M, Molaamin F (2013) Theoretical study of boron nitride nanotubes with armchair forms. Fuller Nanotub Car N 21(5):381–393
38. Schreiner PR, Fokin AA, Pascal RA Jr, de Meijere A (2006) Many density functional theory approaches fail to give reliable large hydrocarbon isomer energy differences. Org Lett 8:3635–3638
39. Zhao Y, Truhlar DG (2006) A density functional theory that accounts for medium-range correlation energies in organic chemistry. Org Lett 8:5753–5755
40. Ao Z, Yang J, Li S, Jiang Q (2008) Enhancement of CO detection in Al doped graphene. ChemPhys Lett 461(4):276–279
41. Kohn W, Sham LJ (1965) Self-consistent equations including exchange and correlation effects. Phys Rev 140:A1133–A1138
42. Perdew JP, Burke K, Ernzerhof (1996) Generalized gradient approximation made simple. Phys Rev Lett 77:3865–3868
43. Blöchl PE, Jepsend O, Andersen OK (1994) Improved tetrahedron method for Brillouin-zone integrations. Phys Rev B 49:16223
44. Besler BH, Merz KM, Kollman PA (1990) Atomic charges derived from semi empirical methods. J Comput Chem 11:431–439. doi:10.1002/jcc.540110404
45. Chirlian LE, Francl MM (1987) Atomic charges derived from electrostatic potentials: a detailed study. J Comput Chem 8:894–905. doi:10.1002/jcc.540080616
46. Brneman GM, Wiberg KB (1990) J Comput Chem 11:361
47. This approach (CHELPG) is shown to be considerably less dependent upon molecular orientation than the original CHELP program. The results are compared to those obtained by using CHELP
48. Martin F, Zipse H (2005) Charge distribution in the water molecule — a comparison of methods. J Comput Chem 26:97–105
49. Monajjemi M, Lee VS, Khaleghian M, Honarparvar B, Mollaamin F (2010) Theoretical description of electromagnetic nonbonded interactions of radical, cationic, and anionic NH2BHNBHNH2 inside of the B18N18 nano ring. J Phys Chem C 114:15315
50. Monajjemi M, Khaleghian M (2011) EPR study of electronic structure of [CoF6] and B18N18 nano ring field effects on octahedral complex. J Clust Sci 22:673–692. doi:10.1007/s10876-011-0414-2
51. Monajjemi M (2012) Quantum investigation of non-bonded interaction between the B15N15 ring and BH2NBH2 (radical, cation, anion) systems: a nano molecular motor. Struct Chem 23:551
52. Balderchi A, Baroni S, Resta R (1998) Phys Rev Lett 61:173
53. Politzer P, Lane P, Murray JS, Concha MC (2005) Comparative analysis of surface electrostatic potentials of carbon, boron/nitrogen and carbon/boron/nitrogen model nanotubes. J Mol Model 1(11):1–7